Received: 2 December 2019 | Revised: 9 December 2019 | Accepted: 20 December 2019

DOI: 10.1002/jmr.2832

RESEARCH ARTICLE

Journal of Molecular Recognition WILEY

Specific monitoring of aflatoxin M1 in real samples using aptamer binding to DNFS based on turn-on method: A novel biosensor

Houman Kholafazad Kordasht[1,2] | Mohammad Hasanzadeh[3]

[1]Nutrition Research Center, Tabriz University of Medical Sciences, Tabriz, Iran

[2]Biotechnology Research Center, Tabriz University of Medical Sciences, Tabriz, Iran

[3]Pharmaceutical Analysis Research Center, Tabriz University of Medical Sciences, Tabriz, Iran

Correspondence
Mohammad Hasanzadeh, Pharmaceutical Analysis Research Center, Tabriz University of Medical Sciences, Tabriz, Iran.
Email: hasanzadehm@tbzmed.ac.ir; mhmmd_hasanzadeh@yahoo.com

Funding information
Tabriz University of Medical Sciences, Tabriz, Iran

Abstract

In the present work, a novel biocompatible scaffold was fabricated for the DNA aptamer immobilization. For the first time, amino-functionalized dendritic fibrous nanosilica (KCC-1-nPr-NH_2) and gold nanoparticle supported by chitosan (AuNPs-CS) were synthesized and electrodeposited successfully on the surface of the glassy carbon electrode by chronoamperometry technique. Unique oligonucleotide of aflatoxin M1 (5′-ATC CGT CAC ACC TGC TCT GAC GCT GGG GTC GAC CCG GAG AAA TGC ATT CCC CTG TGG TGT TGG CTC CCG TAT) labeled by toluidine blue was immobilization on the prepared interface. Hence, a novel aptamer-based bioassay was formed for highly sensitive quantitation of AFM1 using cyclic voltammetry and differential plus voltammetry. The structure and morphology of GQDs-CS/KCC-1-nPr-NH_2 were investigated by Fourier-transform infrared spectroscopy, X-ray diffraction, atomic force, scanning electron microscopy, and energy-dispersive X-ray spectroscopy. The achieved low limit of quantification of apta-assay for detection of AFM1 was 10fM. Also, calibration curve was linear from 0.1μM to 10fM in real samples. The proposed apta-assay has acceptable long-term stability. Designed aptasensor has a lot of remarkable advantages including excellent selectivity, sensitivity, and stability that could be used as facile bio-device for the determination of AFM1 in milk samples.

KEYWORDS

advanced nanomaterials, biosensor, DNA aptamer, graphene quantum dots, nanosilica, toxin

1 | INTRODUCTION

Food contamination refers to the presence of harmful chemicals and microorganisms in food.[1] Microorganisms can contaminant food via product secondary metabolites. The fungi secondary metabolite includes aflatoxins, fumonisins, trichothecenes, ochratoxin A, patulin, and zearalenone. Aflatoxins are produced by a group of molds such as Aspergillus syodotamarty, Aspergillus nasreurosensus, Aspergillus parasiticus, and Aspergillus flavus.[2,3] Aflatoxins were classified in 2B carcinogen category by International Agency for Research on Cancer (IARC).[4] AFM1 is the main hydroxyl metabolite of aflatoxin B1 (AFB1) that is changed by hepatic enzyme of cytochrome P450 in the liver of lactating animals following pasturage of contaminated feeds.[5,6] AFM1 has no sign in food samples. The toxicity of AFM1 has been proven by several investigations on human and laboratory animals.[7] Contaminated milk with AFM1 has several effects on the human healthy, such as hepatic failure,[8] liver cancer,[9] and impaired child growth.[10] US regulations prescribe that the maximum level of AFM_1 should not be higher than 500 ng/kg.[11]

AFM1 was determined by some methods such as thin-layer chromatography (TLC), direct analysis in real-time mass spectrometry (DART-MS), high-performance liquid chromatography (HPLC), and enzyme-linked immunosorbent assay (ELISA), previously.[12–15] These techniques need to more washing steps, requiring expensive materials and equipment, and also, they are time-consuming methods. On the other hand, these methods have low sensitivity.[16] Therefore, new

development is necessary for the rapid and sensitive detection of AFM1 in real samples. One of the important methods is biosensing based on aptamers.[17] Aptasensors are important type of biosensors. Aptasensors are stable over a wide range of pH and reproducible. Furthermore, aptamers show specific affinity to analytes, including proteins, amino acids, virus, low-molecular-inorganic compounds-weight organic, peptides, antibiotics, small ions, and even entire cells via vander Waals forces, hydrogen bonding, and electrostatic interactions.[18,19]

In recent years, the use of nanocatalysts has increased quickly and caused in the advancement of several active and capable nanocatalysts for various procedures. These materials have several advantages over formal catalysts, such as excellent activity and high stability. In addition, metal nanoparticles with a superior support provide a large area for the discovery of novel, highly active nanocatalysts for significant and challenging reactions, which also propose the more advantage of recyclability. Moreover, surface functionalized mesoporous systems have appeared as one of the most significant research areas in the concerning of advanced functional materials. Particularly, Polshettiwar et al reported fibrous nanosilica (KCC-1), with the high surface area (typically >700 m^2/g), broad pore size distribution, large pore size, ease of surface modification, low density, stability, and low toxicity with good biocompatibility. This dendritic fibrous nanosilica showed special activities in vast fields such as heterogeneous catalysis, gas capture, solar energy harvesting, energy storage, medical diagnosis, targeting of drugs, DNA adsorption, drug delivery applications, bio sensing, and CO_2 mitigation.[20,21]

Nowadays, electrochemical aptasensors with various nanoparticles (NPs) have many benefits such as sensitivity, easy to use, and low cost. In the present study, a novel electrochemical platform was developed for the detection of AFM1 in the milk samples. For this purpose, KCC-1-nPr-NH_2-DPA and AuNPs-CS were synthesized and electrodeposited on the surface of glassy carbon electrode (GCE) by chronoamperometry technique. Then gold NPs were coated on the surface of the electrode. Finally, oligonucleotide was immobilized, and ultrasensitive technique was used for the monitoring of AFM1 in real samples.

2 | EXPERIMENTAL

2.1 | Chemical and reagents

All chemicals were obtained from Sigma-Aldrich (Ontario, Canada) in analytical grade. The oligonucleotide AFM_1 was perturbed from Takapouzist Co (Iran). All cell lines were provided from National Cell Bank of Iran (NCBI) (Tehran, Iran).

2.2 | Synthesis of nanomaterials

2.2.1 | The synthesis of KCC-1-nPr-NH_2-DPA and Au NPs-CS

KCC-1 was synthesized and functionalized according to the previous reports.[20,21]

The AuNPs-CS was provided by 0.005-g CS dissolved in 0.1M acetic acid. Then, the solution was mixed with 10 mL of H_2SO_4 (500mM). Finally, 2 mL of hydrogen tetrachloroaurate (III) hydrate was added to the above solution. Scheme 1 shows synthesized procedure of KCC-1-nPr-Nh2-DPA.

2.3 | Viability study

2.3.1 | Cell culture and MTT test assay

MCF 7 cancer cells were seeded to a 25-mL flask in Roswell Park Memorial Institute 1640 (RPMI) media supplemented with 1% streptomycin/penicillin and 10% FBS at 37°C under 5% of CO_2 atmosphere for at least 72 hours. Next, media of flask was discarded and washed with phosphate buffer solution (PBS) to wash out the excess RPMI. Then, about 30 μL of trypsin-EDTA solution was added and incubated for about 5 minutes at 37°C under 5% atmosphere of CO_2 to separate MCF 7 cells. After that, MCF 7 cancer cells were moved to a 15-mL tube and then centrifuged at 1500 rpm for 5 minutes to remove unreacted trypsin-EDTA molecules. Finally, MCF 7 cells were resuspended to the fresh medium.

Viabilities of KCC-1-nPr-NH_2-DPA-treated MCF 7 cancer cells were evaluated as follows. Firstly, MCF 7 cells (10^{+4} cell/mL) were added to each wells of a 96-well texture plate and were incubated for at least 24 hours to attach and cover at about 40% of each well. Then, wells were treated with different concentrations of KCC-1-nPr-NH_2-DPA nanocomposite and incubated for 72, 48, and 24 hours. Afterwards, about 20 μL of MTT reagent (3.0 mg/mL) was added to wells and incubated for another 4 hours at 37°C under 5% atmosphere of CO_2. After that, media were discarded, and 200 μL of DMSO was added to each well and then incubated for about 30 minutes. Finally, the absorbance of wells was measured at 570 nm, and the viability percent was calculated as follows.

$$\%viability\ of\ cells = \frac{(absorbance_{sample} - absorbance_{blank})}{(absorbance_{control} - absorbance_{blank})} \times 100.$$

3 | RESULT AND DISCUSSION

3.1 | The MTT result of KCC-1-nPr-NH_2-DPA

The cell viability of KCC-1-nPr-NH_2-DPA was studied according to the MTT assay guidelines. The cytotoxicity results of KCC-1-nPr-NH_2-DPA affected MCF 7 cancer cells were tested at incubation time of 24, 48, and 72 hours with various concentrations ranging from 1 to 50 mg/L. As result showed that the MCF 7 cancer cells viabilities of KCC-1-nPr-NH_2-DPA treated were higher than 80% showing the nontoxic nature of KCC-1-nPr-NH_2-DPAparticles towards cancer cells (Figure S1).

3.2 | Characterization of synthesized nanocomposites

As can be seen in Figure S2, TEM images show dendritic structure of fibrous nanosilica. The presence of numerous lateral branches leads to increased solubility and fluidity. As the images were proven, these materials have high uniform structure. Also, FE-SEM images of KCC-1, KCC-1-nPr-NH_2, and KCC-1-nPr-NH_2-DPA were shown in Figure S3. The images show that all of three compounds consist of spheres. Furthermore, because of dendrimer structure, these materials have high surface area. The EXS result confirmed FESEM (Figure S4C).

FTIR was applied to approve the proper functionalization of the KCC-1 with –NH_2. As shown in Figure S5, the characteristic peaks of the silica-based materials could be observed in the range of 1020 to 1110 cm^{-1} representing the Si–O–Si asymmetric stretching. Also, Si–OH peak is observed at 960 cm^{-1}.

The BJH and BET analyses of KCC-1, KCC-1-nPr-NH_2, and KCC-1-nPr-NH_2-DPA were examined to authenticate the mesoporous structure of the synthesized materials (Figure S6). According to the obtained results, synthesized silica materials have mesoporous structure. Furthermore, the adsorption isotherm was used for the investigation of specific surface area and porosity of the synthesized materials. For calculation of the pore volume of nanosilica, BET and BJH were used. Table 1 shows the surface area, pore size, and pore volume of KCC-1, KCC-1-nPr-NH_2, and KCC-1-nPr-NH_2-DPA. The surface area of KCC-1 changed from 713 m^2/g to 467 and 78.2 m^2/g for KCC-1-nPr-NH_2 and KCC-1-nPr-NH_2-DPA, respectively. And, the pore volumes were 1.4 to 1.1 and 1.22 cm^3/g for KCC-1, KCC-1-nPr-NH_2, and KCC-1-nPr-NH_2-DPA. Also, pores were 8.9, 10.4, and 7.6 for KCC-1, KCC-1-nPr-NH_2, and KCC-1-nPr-NH_2-DPA, respectively.

TABLE 1 Analytical figure for quantification of AFM1 by various electrochemical aptasensors

Assay Strategy	LOD	Dynamic Range	Ref
Label-free aptamer-AFM1 on Fe3O4/PANi	1.98 ng/L	6-60 ng/L	22
DNA-aptamers immobilized on a carbon screen-printed electrode	1.15 ng/L	2-150 ng/L	23
Apt-modified SPGE with CS-modified AUNPs	0.9 ng/L	2-600 ng/L	24

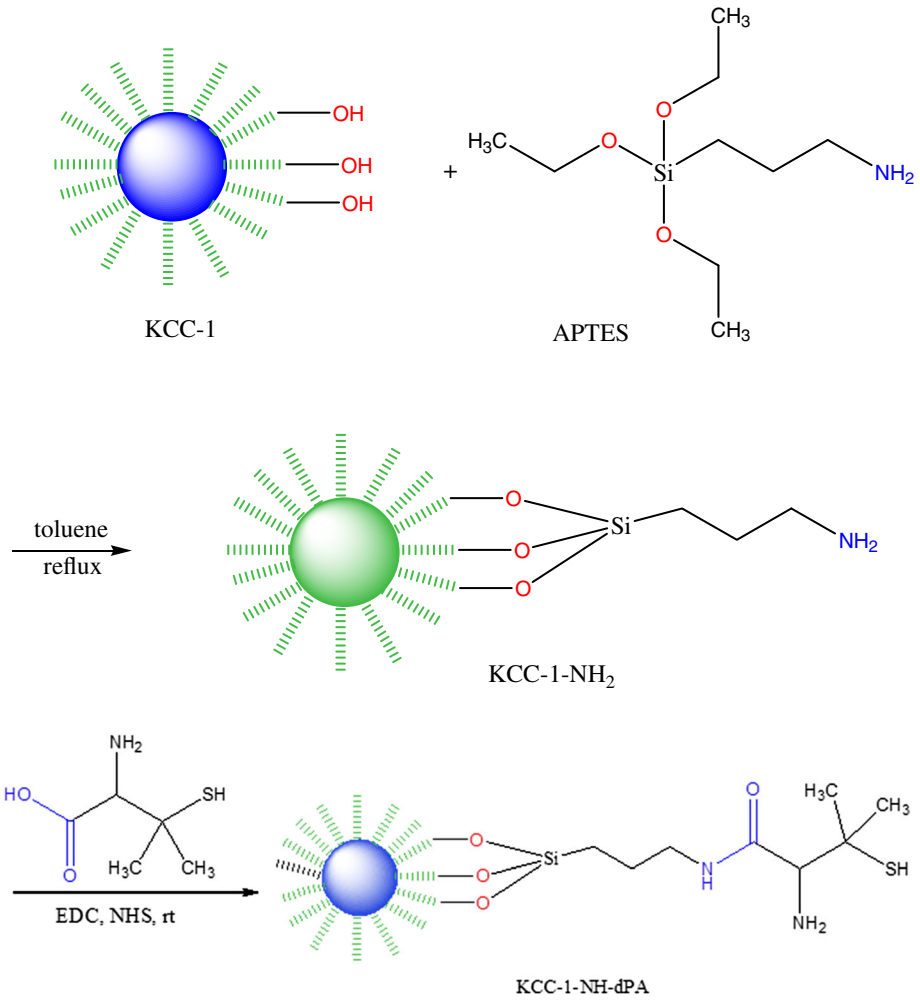

SCHEME 1 Synthesized procedure of KCC-1-nPr-NH_2-DPA

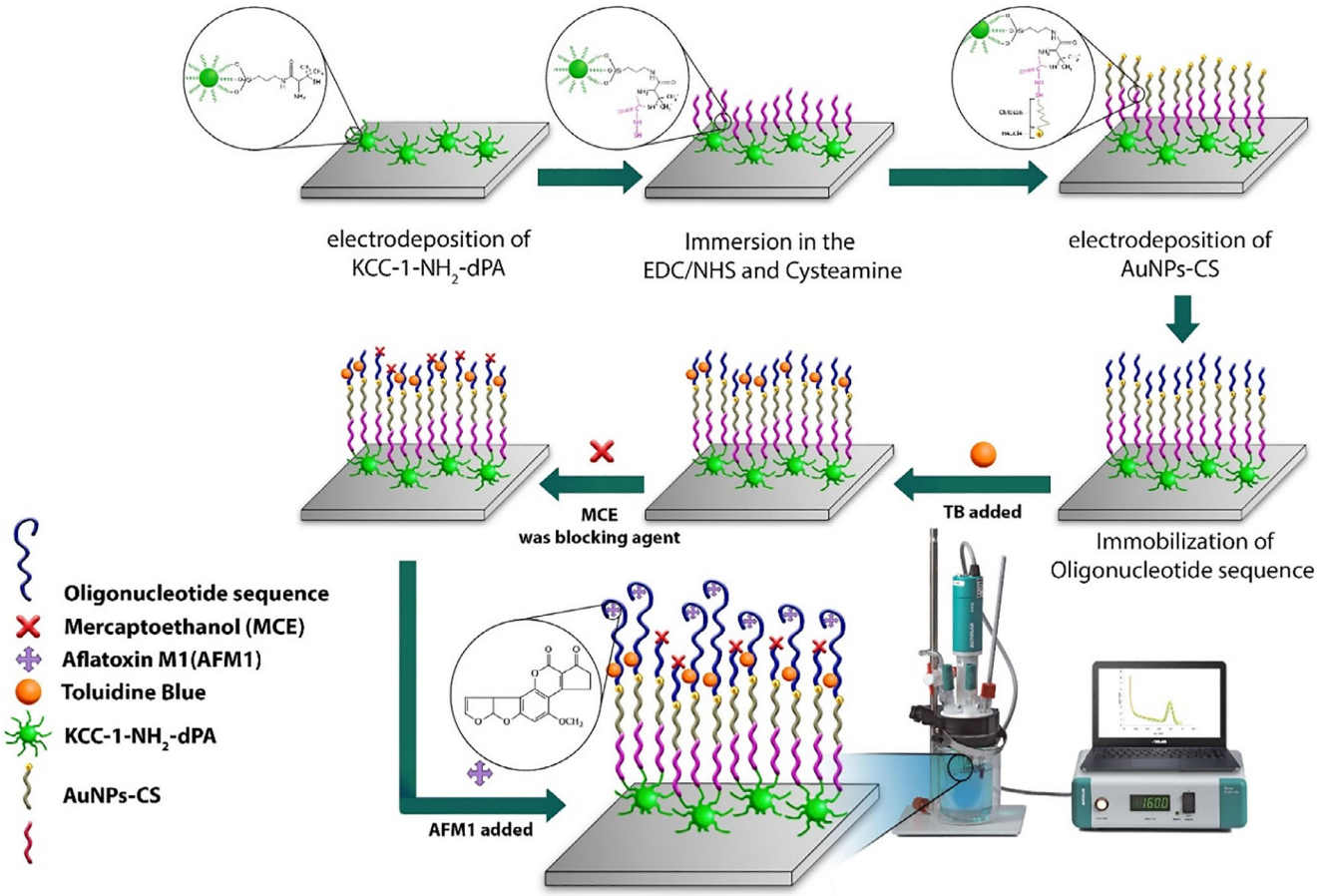

SCHEME 2 Fabrication of aptasensor for detection of AFM_1

The XRD patterns of KCC-1, KCC-1-nPr-NH_2, and KCC-1-nPr-NH_2-DPA were carried out from 3.0° (2θ) to 70.0° (2θ) (Figure S7). As can be seen, the result indicated that crystallinity was increased from KCC-1 to KCC-1-nPr-NH_2-DPA, which is because of two significant peaks. The wide peak for 20° and 30° is conformed amorphous structure of silica.

3.3 | Electrodeposition of KCC-1-nPr-NH_2-DPA and AuNPs-CS

For this purpose, GCE was completely polished with 0.05-μm alumina. Afterward, the electrode was sonicated with 1:1 alcohol (v/v), acid nitric, and deionized water. Finally, GCE was dried at room temperature. So, KCC-1-nPr-NH_2-DPA was electrodeposited on the surface of GCE by ChA technique (Figure 1A). Then the GCE coated by KCC-1-nPr-NH_2-DPA was incubated with EDC/NHS aqueous solution for 20 minutes. The KCC-1-nPr-NH_2-DPA was activated by EDC/NHS by coupling between (SH and NH_2) group of KCC-NH_2-DPA and carboxylate group of EDC/NHS. So, the electrode was washed by deionized water. The electrode was immersed in the cysteamine (0.1M) aqueous solution for 1 hour. The NH and SH groups of cysteamine were bind with active surface of electrode (Scheme 2). The ChA technique was employed for the electrodeposition of AuNPs-CS on the surface of engineered electrode (Figure 1B).

3.4 | Aptamer immobilization

The oligonucleotide aptamer was immobilized on the surface of GCE modified by KCC-NH_2-DPA. For this purpose, the unique oligonucleotide was diluted in 500-μL Tric-HCL buffer and mixed with 5 μL of TB (20μM), which was used as indicator. Then, the 10 μL of aptamer was immobilized on the surface of electrode and incubated at −4°C for 6 hours. So, MCH as blocking agent was added to the substrate of the electrode to reduce nonspecific adsorption for 20 minutes. Scheme 1 summarized all of the fabrication steps of aptasensor.

3.5 | Characterization of the engineered surface

FE-SEM and EDX were applied for the analysis of morphology and structure of modified surface. Figure 2 demonstrated FESEM images of KCC-1-nPr-NH_2-DPA/GCE, KCC-1-nPr-NH_2-DPA-Cys A/GCE,

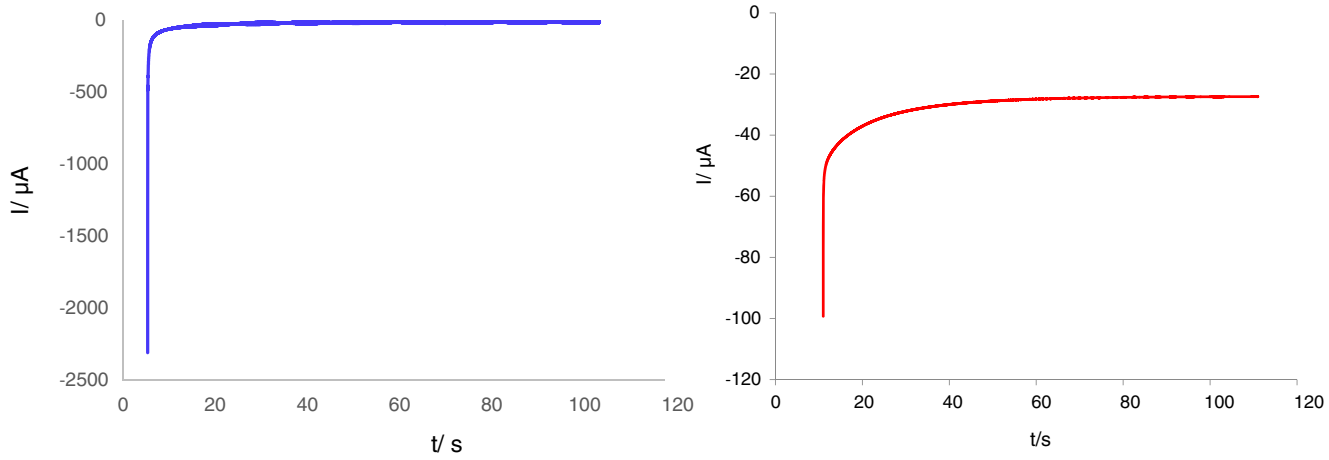

FIGURE 1 (A) ChA of KCC-1-nPr-NH_2-DPA (0.01 g in the deionized water) at the potential of −0.24 V during 100 seconds. (B) ChA of the solution containing $HAuCl_4$ (500mM) in the present of CS (0.005 g in the 0.1M acetic acid) at the potential of 0 V during 100 seconds

KCC-1-nPr-NH_2-DPA-Cys A-AuNPs/GCE, and KCC-1-nPr-NH_2-DPA-Cys A-AuNPs-Aptamer/GCE (Figure 9A-D), respectively. According to obtained results, all of the deposition and immobilization steps were done successfully.

3.6 | Electrochemical behavior of aptasensor

Nowadays, CVs is extremely useful technique for the investigation of prepared surfaces. In the present study, aptasensor preparation steps were clearly investigated via CV technique in 0.01M ferrocyanide/ferricyanide solution (Figure 3). The obtained result indicates that, when the GCE was modified by KCC-1-nPr-NH_2-DPA, the peak current was increased lowly. But, after modification by AuNPs-CS, the peak current was increased dramatically. After immobilization of aptamer, the peak currents of KCC-1-nPr-NH_2-DPA-Cys A-AuNPs-Aptamer was decreased, which confirmed successful proportion of aptasensor.

3.7 | Kinetic study

CV techniques applied for the investigated electrochemical behavior of KCC-1-nPr-NH_2-DPA-CysA-AuNPs-CS in different scan rates (10-500 mV/s) in 0.01M $[Fe(CN)_6]^{3-/4-}$ (Figure S8A). As can be seen, the peak currents of CV curve were increased by increasing scan rate. Also in the slow sweep rates, the electron exchange happened slowly at the surface of electrode leading to narrower voltammogram with lower peak current. Furthermore, the value of R^2 for linear regression in different scan rate is 0.9847 (Figure S8B).

3.8 | Analytical behavior

After detection of AFM1 using propose aptasensor, DPV and SWV techniques were applied to the demonstration of different concentration of AFM1 (0.1µM to 10fM) under optimal conditions in 0.01M ferrocyanide/ferricyanide solution. These techniques have several abilities, including lower background current, high current sensitivity, and low signal to noise in distinction than CV technique. Figure 4A,B demonstrated the CVs, DPVs, SWVs, and calibration curves at different concentration of AFM1. As can be seen, generally with decrease of AFM1 concentration, the oxidant peak currents of DPV, SWV, and CV were increased. On the other hand, according to R^2 ($R^2_{CV} < R^2_{DPV} < R^2_{SWV}$), SWV is the most accurate technique for the determination of AFM1. As expected, sensitivity of SWV and DPV techniques is more than CV technique. According to the obtained result, linear range was 10fM to 0.1µM, which LLOQ obtained as 10fM. Analytical performance of this biosensor was compared with previously reported aptasensor (Table 1). According to obtained results, the engineered aptasensor based on KCC-1-nPr-NH_2-DPA was used for the determination of AFM1 in milk samples.

3.9 | Real sample analysis

DPV and SWV techniques were applied for the monitoring of AFM1 in the pasteurized milk (Figure 4C). As above mentioned, the 0.01M ferrocyanide/ferricyanide solution was chosen as the supporting electrolyte for the quantification of AFM1 in the milk samples. Before the experiment was started, the spiked milk was prepared with different concentration of AFM1. Hence, 10 µL of spiked milk samples with different concentration of target were incubated on the engineered

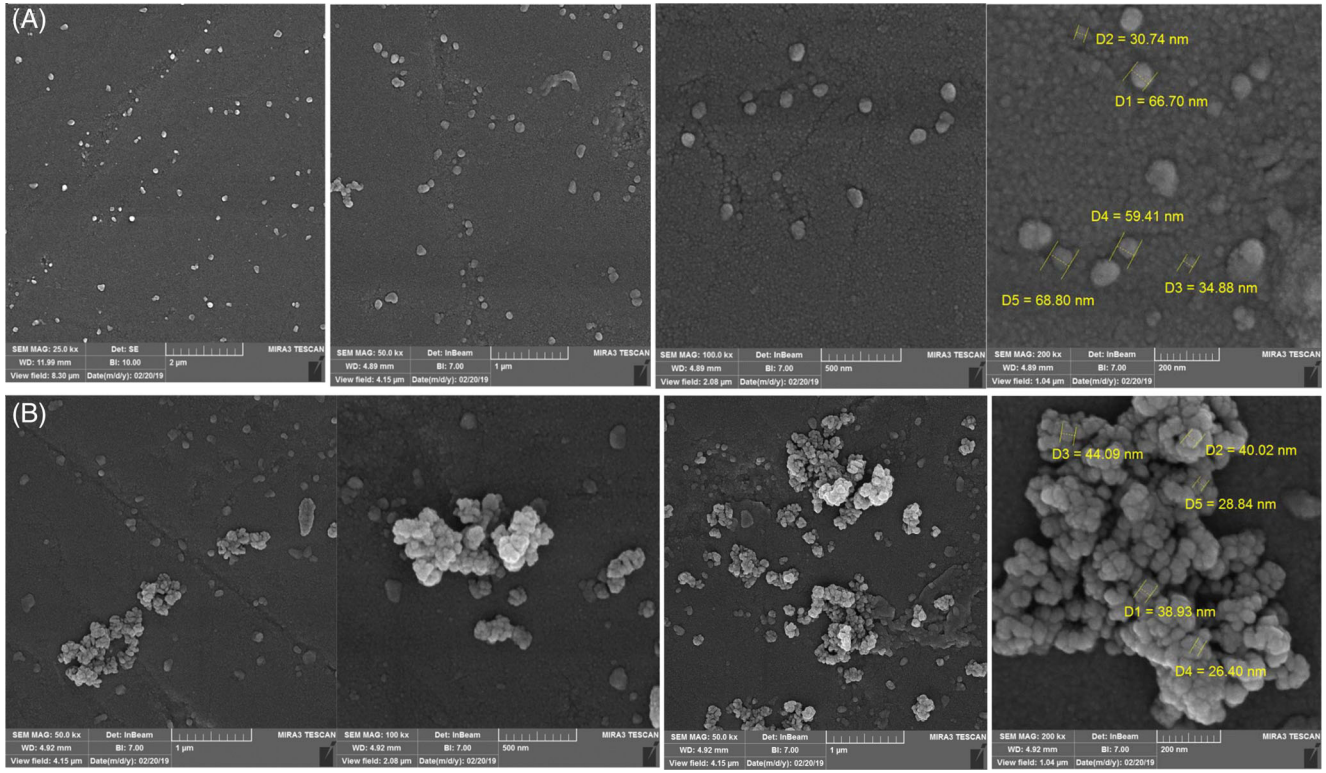

FIGURE 2 The FE-SEM images of GCE modified by (A) KCC-1-nPr-NH_2-DPA. (B) KCC-1-NH_2-DPA-Cys A. (C) KCC-1-nPr-NH_2-DPA-Cys A-AuNPs-CS. (D) Electrode- KCC-1-nPr-NH_2-DPA-Cys A-AuNPs-CS-Apt in the different magnification

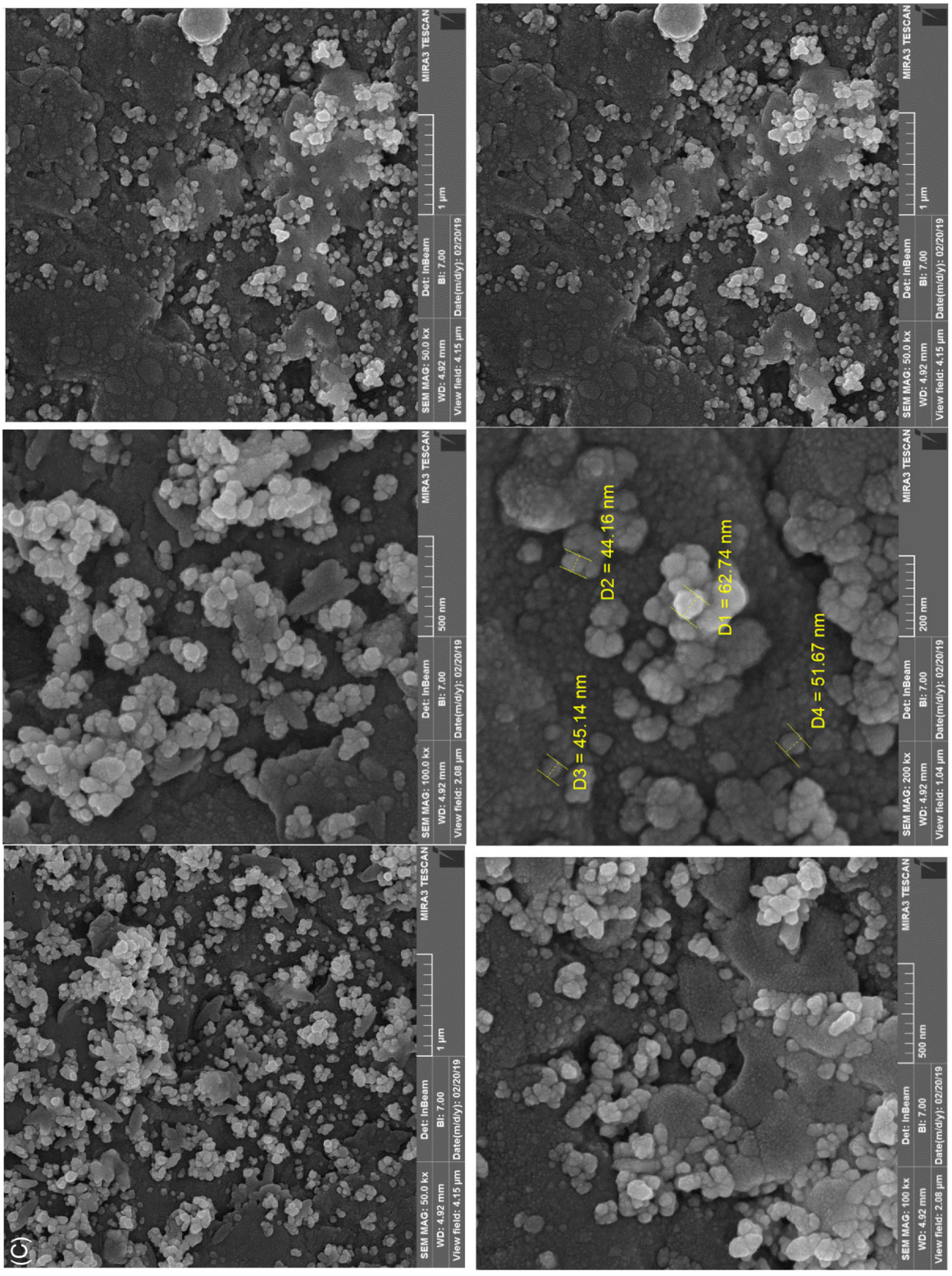

FIGURE 2 (Continued)

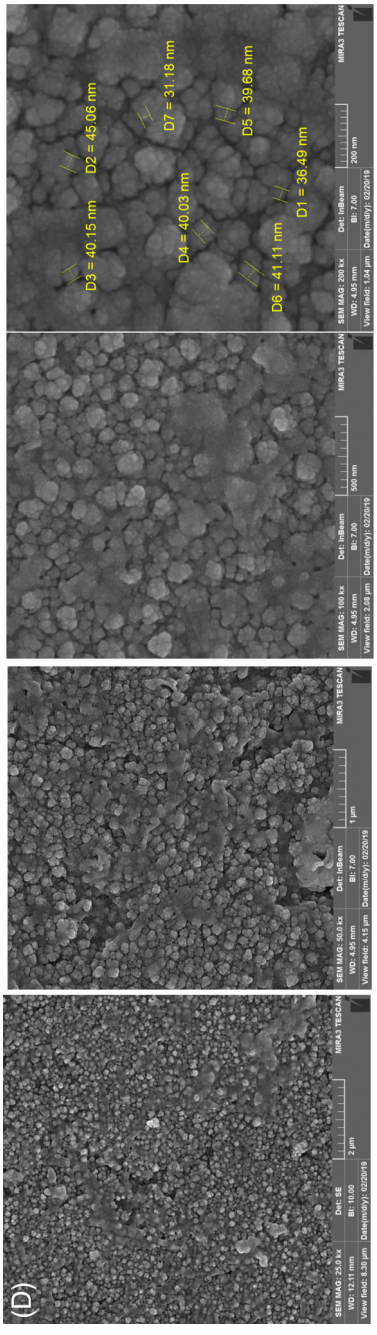

FIGURE 2 (Continued)

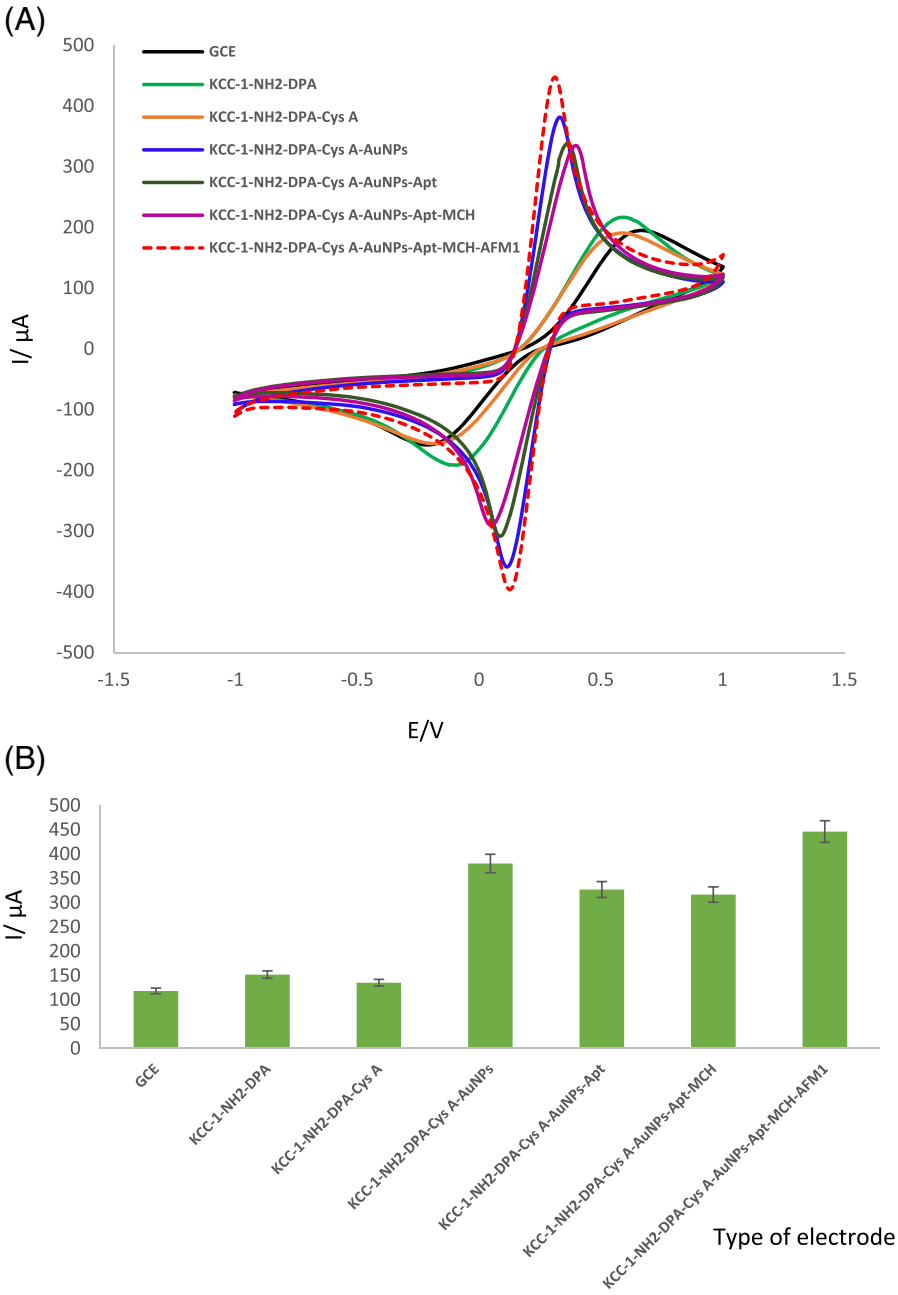

FIGURE 3 (A) CVs of bare GCE and GCE modified by KCC-1-nPr-NH_2-DPA, KCC-1-NH_2-DPA-Cys A, KCC-1-nPr-NH_2-DPA-Cys A-AuNPs-CS, KCC-1-nPr-NH_2-DPA-Cys A-AuNPs-CS-Apt, KCC-1-nPr-NH_2-DPA-Cys A-AuNPs-CS-Apt-MCH, and KCC-1-nPr-NH_2-DPA-Cys A-AuNPs-CS-Apt-MCH-AFM1 in 0.01M $[Fe(CN)6]^{3-/4-}$ at the −1 to +1 V. (B) Histogram of electrochemical behaviors for the step by step preparation

surface. Then, DPVs and SWVs were recorded under optimal conditions. Also the LLOQ for both of them was 10fM.

3.10 | Assessment of stability

Stability is an important factor on the evaluation of the biosensor performance. Figure S8C shows CVs of GCE modified by KCC-NH_2-DPA in different cycle number. As can be seen, with the increase of the cycle numbers to 100, peak current was not changed, which confirmed high stability of the prepared interface.

The stability of the engineered aptasensor is extremely significant for practical application. Assessment of the stability test was done in the different period times by recording CVs in 0.01M ferrocyanide/ferricyanide solution. According to the obtained results, designed aptasensor has excellent stability till 4 days (Figure S9).

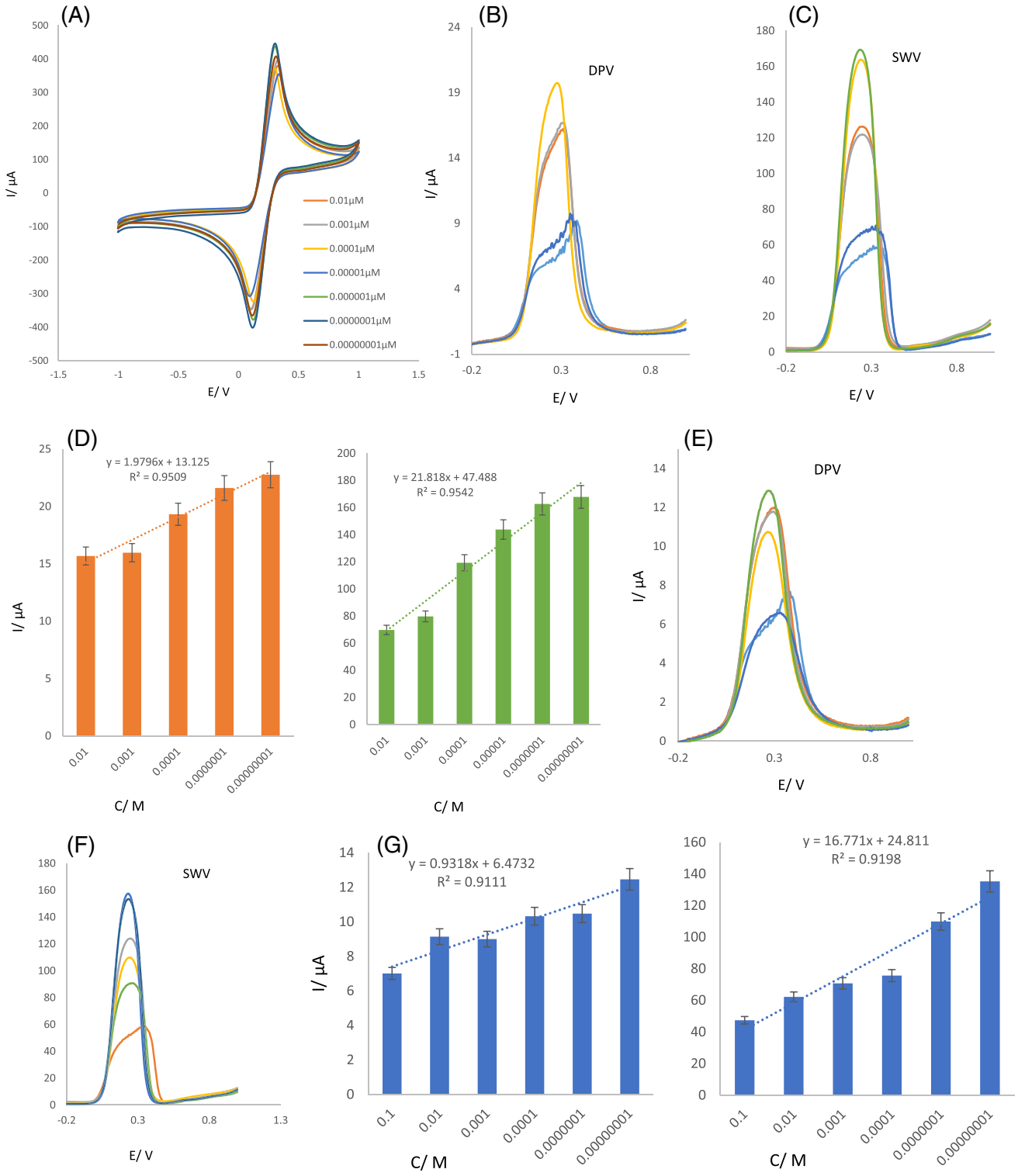

FIGURE 4 (A) The CVs of the KCC-1-nPr-NH_2-DPA-Cys A-AuNPs-CS-Apt in different concentration of AFM1 (0.1µM-1fM) (B) Calibration curve (B and C) DPVs and SWVs of KCC-1-nPr-NH_2-DPA-Cys A-AuNPs-CS-Aptamer in different concentration of AFM_1. (D) Calibration curve. (E and F) DPVs and SWVs of KCC-1-nPr-NH_2-DPA-Cys A-AuNPs-CS-aptamer in the different concentration of AFM_1 spiked in pasteurized milk. (G) Calibration curve

4 | CONCLUSION

An innovative electrochemical aptasensor was developed for the detection and determination of AFM1 using KCC-1-nPr-NH_2-DPA. For this purpose, KCC-1-nPr-NH_2-DPAwas synthesized and electrodeposited on the surface of GCE by ChA technique. Afterward, the gold NPs supported by CysA electrodeposited on the surface of modified electrode. Finally, the especially oligonucleotide tagged TB

(as indicator) was immobilized on the surface of the electrode. The linear concentration and calibration curve was monitored in the range of 0.1μM to 10fM, which LLOQ was 10 fM. Finally, this high selectivity, rapid, and accurate aptasensor was successfully used for the detection of AFM1 in milk samples.

ACKNOWLEDGEMENT

This study was funded by Tabriz University of Medical Sciences, Tabriz, Iran.

CONFLICT OF INTEREST

All the authors (H. Kholafazad Kordasht and M. Hasanzadeh) have read, approved, and made substantial contributions for the manuscript. None of the original material contained in this manuscript has been previously published nor is currently under review for publication elsewhere. Besides, authors declare no conflict of interests and/or commercial products or companies.

ORCID

Mohammad Hasanzadeh https://orcid.org/0000-0003-4918-1239

REFERENCES

1. Manning L, Baines R, Chadd S. *Deliberate contamination of the food supply chain*. Br Food J. 2005;107:225-245.
2. Cavalheiro AC. *Aflatoxin and Aflatoxicosis—a review*. Worlds Poult Sci J. 1981;37:34-38.
3. Creppy EE. *Update of survey, regulation and toxic effects of mycotoxins in Europe*. Toxicol Lett. 2002;127:19-28.
4. IARC Working Group on the Evaluation of Carcinogenic Risks to Humans. Some traditional herbal medicines, some mycotoxins, naphthalene and styrene, World Health Organization; 2002.
5. Cathey C, Huang Z, Sarr A, Clement B, Phillips T. *Development and evaluation of a minicolumn assay for the detection of aflatoxin M1 in milk*. J Dairy Sci. 1994;77:1223-1231.
6. Moosavy M-H, Hasanzadeh M, Soleymani J, Mokhtarzadeh A. *Determination of aflatoxin M1 using an aptamer-based biosensor immobilized on the surface of dendritic fibrous nano-silica functionalized by amine groups*. Anal Methods. 2019;11:3910-3919.
7. Bahrami R, Shahbazi Y, Nikousefat Z. *Aflatoxin M1 in milk and traditional dairy products from west part of Iran: occurrence and seasonal variation with an emphasis on risk assessment of human exposure*. Food Control. 2016;62:250-256.
8. Asim M, Sarma MP, Thayumanavan L, Kar P. *Role of aflatoxin B1 as a risk for primary liver cancer in north Indian population*. Clin Biochem. 2011;44:1235-1240.
9. Hamid AS, Tesfamariam IG, Zhang Y, Zhang ZG. *Aflatoxin B1-induced hepatocellular carcinoma in developing countries: geographical distribution, mechanism of action and prevention*. Oncol Lett. 2013;5:1087-1092.
10. Egal S, Hounsa A, Gong Y, et al. *Dietary exposure to aflatoxin from maize and groundnut in young children from Benin and Togo, West Africa*. Int J Food Microbiol. 2005;104:215-224.
11. Afkhami A, Hashemi P, Bagheri H, Salimian J, Ahmadi A, Madrakian T. *Impedimetric immunosensor for the label-free and direct detection of botulinum neurotoxin serotype a using au nanoparticles/graphene-chitosan composite*. Biosens Bioelectron. 2017;93:124-131.
12. Kim E, Shon D, Ryu D, Park JW, Hwang H, Kim Y. *Occurrence of aflatoxin M1 in Korean dairy products determined by ELISA and HPLC*. Food Addit Contam. 2000;17:59-64.
13. Rodriguez Velasco M, Calonge Delso M, Ordonez Escudero D. *ELISA and HPLC determination of the occurrence of aflatoxin M 1 in raw cow's milk*. Food Addit Contam. 2003;20:276-280.
14. Busman M, Bobell JR, Maragos CM. *Determination of the aflatoxin M1 (AFM1) from milk by direct analysis in real time–mass spectrometry (DART-MS)*. Food Control. 2015;47:592-598.
15. Shundo L, Sabino M. *Aflatoxin M1 in milk by immunoaffinity column cleanup with TLC/HPLC determination*. Braz J Microbiol. 2006;37:164-167.
16. Lim Y, Kouzani A, Duan W. *Aptasensors: a review*. J Biomed Nanotechnol. 2010;6:93-105.
17. Mirzaie A, Hasanzadeh M, Jouyban A. *Cross-linked chitosan/thiolated graphene quantum dots as abiocompatible polysaccharide towards aptamer immobilization*. Int. J. Biological Macromol. 2019;123:1091-1105.
18. Citartan M, Gopinath SC, Tominaga J, Tan S-C, Tang T-H. *Assays for aptamer-based platforms*. Biosens Bioelectron. 2012;34:1-11.
19. Karczmarczyk A, Baeumner AJ, Feller K-H. *Rapid and sensitive inhibition-based assay for the electrochemical detection of Ochratoxin A and Aflatoxin M1 in red wine and milk*. Electrochim Acta. 2017;243:82-89.
20. Polshettiwar V, Cha D, Zhang X, Basset JM. *High-surface-area silica nanospheres (KCC-1) with a fibrous morphology*. Angew Chem Int Ed. 2010;49:9652-9656.
21. Mahmudi M, Shadjou N, Ahour F, Hasanzadeh M. *Synthesis and adsorption behavior of dendritic Fibrous Nano-silica (DFNS) grafted by d-penicillamine as an advanced nanomaterial for the removal of some metal ions from contaminated water*. J Electroanal Chem. 2019;848:113272.
22. Vural T, Yaman YT, Ozturk S, Abaci S, Denkbas EB. *Electrochemical immunoassay for detection of prostate specificantigen based on peptide nanotube-gold nanoparticle-polyaniline immobilizedpencil graphite electrode*. J Colloid Interface Science. 2018;510:318-326.
23. Maehashi K, Okuno J, Matsumoto K, Kerman K, Takamura Y, Tamiya E. *Label-Free Amperometric Biosensors Based on Single-Walled Carbon Nanotube Modified Microelectrodes*. Paper presented at: 2006 64th Device Research Conference 2006.
24. Kong R-M, Ding L, Wang Z, You J, Qu F. *Anovel aptamer-functionalized MoS 2 nanosheet fluorescent biosensor forsensitive detection of prostate specific antigen*. Analytical Bioanalytical chemistry. 2015;407(2):369-377.

SUPPORTING INFORMATION

Additional supporting information may be found online in the Supporting Information section at the end of this article.

How to cite this article: Kordasht HK, Hasanzadeh M. Specific monitoring of aflatoxin M1 in real samples using aptamer binding to DNFS based on turn-on method: A novel biosensor. *J Mol Recognit*. 2020;e2832. https://doi.org/10.1002/jmr.2832